Peer-reviewed version available at Cancers 2019, 11, 784; doi:10.3390/cancers11060784

Article

NGF Induces Proliferation and Aggressiveness in Prostate Cancer Cells.

Marzia Di Donato [1], Gustavo Cernera [1], Antimo Migliaccio[1]* and Gabriella Castoria[1]*

[1] Department of Precision Medicine - University of Campania 'L. Vanvitelli' - via L. De Crecchio, 7- 80138 Naples (Italy)

* Correspondence: gabriella.castoria@unicampania.it (G.C.)
antimo.migliaccio@unicampania.it (A.M.)

Abstract: Resistance to hormone therapy and disease progression is the major challenge in clinical management of prostate cancer (PC). Drugs currently used in PC therapy initially show a potent antitumor effect. Nevertheless, PC gradually develops resistance, relapses and spreads. Most patients develop, indeed, castrate-resistant PC (CRPC), which is almost incurable.

The nerve growth factor (NGF) acts on a variety of non-neuronal cells by activating the NGF tyrosine-kinase receptor, TrkA. NGF signaling is deregulated in PC. In androgen-dependent PC cells, TrkA mediates the proliferative action of NGF through its cross talk with the androgen receptor (AR). Epithelial PC cells, however, acquire the ability to express NGF and TrkA, as the disease progresses, indicating a role for NGF/TrkA axis in PC progression and androgen-resistance.

We here report that once activated by NGF, TrkA mediates proliferation, invasiveness and epithelial-mesenchyme transition (EMT) in various CRPC cells. NGF promotes organoid growth in 3D models of CRPC cells, and specific inhibition of TrkA impairs all these responses. Thus TrkA represents a new biomarker to target in CRPC.

Keywords NGF/TrkA signaling, mitogenesis, invasiveness, EMT, 3D models, castrate-resistant prostate cancers.

1. Introduction

PC is the most commonly diagnosed non-cutaneous tumor in men and the second leading cause of male cancer-related deaths in Western society [1]. This cancer is often characterized by a slow and symptom-free growth, and early-stage treatments include radical prostatectomy, novel androgen receptor (AR) pathway inhibitors, such as abiraterone and enzalutamide, external beam radiotherapy (RT), brachytherapy and cryotherapy [2, 3]. Further, use of new tracers for PET/TC [4–7] and novel focal therapies [8, 9] have provided important advances in diagnosis, follow-up and treatment of PC patients in the last decade.

The role of steroid hormones, mainly the androgens, in prostate transformation and PC progression is well established and molecular studies have extensively analysed the mechanism of AR or estrogen receptors (ERs) action in PC. These studies have made it possible the synthesis of new drugs that modulate or inhibit the biological events induced by sex steroid receptors (SRs) in PC cells [10–15]. The long-term efficacy of these drugs, however, still remains unsatisfactory and novel therapeutic approaches are needed to limit PC progression and inhibits metastasis occurrence.

Peer-reviewed version available at Cancers 2019, 11, 784; doi:10.3390/cancers11060784

Receptor tyrosine kinases (RTKs) drive prostate transformation and PC progression [16]. Among them, the tropomyosin receptor kinase A (TrkA) binds NGF thereby activating Ras/MAPK, PI3-K and PLCγ signaling pathways to promote survival, proliferation and invasiveness of cells [17, 18]. The human prostate releases abundant levels of NGF [19], which, in turn, controls the normal development of prostate tissue [20]. Specifically, the stromal cells secrete NGF, which binds to TrkA and p75NTR expressed in the epithelial counterpart, stimulating its growth [21–23]. Moreover, preclinical studies have highlighted the role of NGF/TrkA signalling in PC proliferation and metastasis [24–30]. Molecular changes in epithelial or stromal cells lead to the paracrine and/or autocrine production of NGF, thus promoting prostate carcinogenesis. Simultaneously, a persistent expression of TrkA, together with the loss of expression of p75NTR receptors, is often detected in PC patients [26]. As such, PC cells might exclusively utilize NGF signaling to survive. Noticeably, we have recently shown that a cross talk between TrkA and AR modulates the NGF action in quite divergent cell types. Such intersection controls the androgen-elicited differentiation in neuronal-derived cells [31], while it controls the NGF-induced proliferation and migration in androgen-sensitive LNCaP cells [32]. Therefore, TrkA represents a promising new 'druggable' biomarker in prostate proliferative diseases [33].

Despite the accumulating evidence, the mechanism(s) leading to derangement of TrkA signaling in CRPC remains, however, poorly understood and genetic screening did not reveal TrkA mutations or Trk-fusion onco-proteins in PC patients [34, 35]. These findings further reinforce the concept that derangement of an intact NGF/TrkA signaling may be involved in PC progression.

In this study, we have used C4-2B [36, 37], PC3 [38] and DU145 [39] cell lines, which derive from CRPC and express at different extent TrkA [40]. C4-2B cells are also positive for AR [41], while PC3 and DU145 cells are both negative for AR [42, 43]. Additionally, all the cell lines express ERβ, while they do not express ERα. In these cell lines, we have analysed the effects of NGF, alone or in combination with its specific inhibitor GW441756 [44] on cell proliferation, migration, invasiveness and EMT by analysing BrdU incorporation, cell motility, invasiveness and EMT markers. Analysis of the pathways implied in NGF signalling is also reported, pointing to the key role of MAPK as well as Akt activation in the observed effects. At last, a study in 3D model further corroborates the finding that inhibition of TrkA impairs the NGF-elicited growth of organoids derived from CRPC cells.

2. Results

2.1 The mitogenic effect of NGF in CRPC cells.

Expression of TrkA as well as SRs in CRPC-derived C4-2B, DU145 and PC3 cells was analyzed by Western blot technique (Fig 1A). The anti-TrkA antibody revealed a 140 KDa band in lysates from cell lines used. Of note, the amount of TrkA expressed in DU145 was higher than that observed in C4-2B and PC3 cells. Only C4-2B cells express AR. ERα was undetectable in all CRPC cell lines, while it was revealed in lysate proteins from breast cancer MCF-7 cells, used as positive control. Albeit at different extent, all the CRPC cell line used express ERβ. Lysates proteins were also analyzed for E-cadherin and vimentin expression, as epithelial or mesenchyme marker, respectively.

Even though at different extent, C4-2B, DU145 and PC3 cells express high levels of E-cadherin and low levels of vimentin (Fig. 1A), indicating the epithelial signature of cell lines here employed.

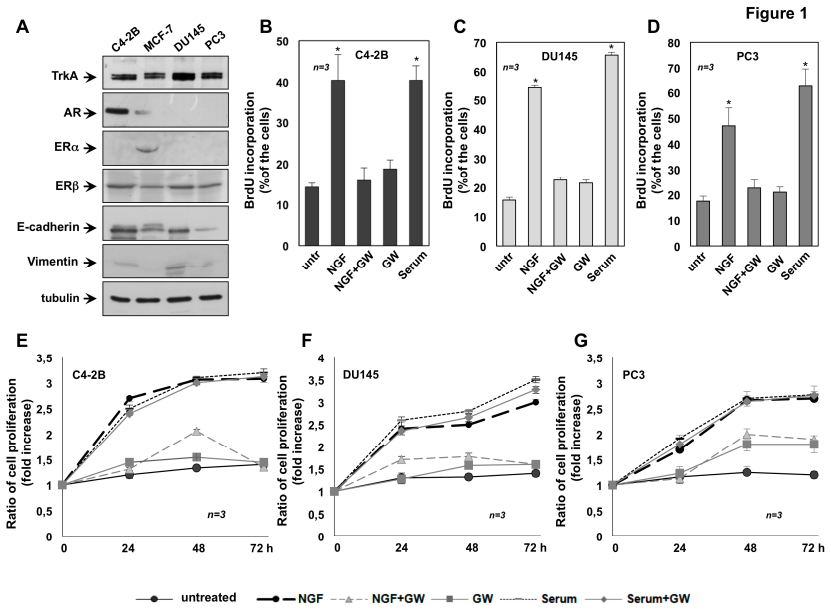

Figure 1. TrkA activation mediates the NGF mitogenic effect in CRPC cells. C4-2B, DU145 and PC3 cells were used. In **A**, lysates from the indicated cell lines were prepared and proteins were analyzed by Western blot, using the antibodies against the indicated proteins. Quiescent C4-2B (**B**), DU145 (**C**) and PC3 (**D**) cells were left untreated (untr) or treated for 18h with the indicated compounds. After *in vivo* pulse with 100 μM BrdU, BrdU incorporation was analyzed by IF and expressed as % of total cells. Quiescent C4-2B (**E**), DU145 (**F**) and PC3 (**G**) were left untreated or treated for 24, 48 and 72 h with the indicated compounds. Cell proliferation was assayed using the WST-1 reagent. Graphs in **E-G** represent the ratio of proliferation, which was expressed as fold increase over the basal absorbance. NGF stimulation induced a significant variation of the proliferation as compared with untreated cells ($p < 0,05$). In **B-G,** NGF was used at 100 ng/ml; GW441756 (GW) was used at 1μM. When indicated, serum was used at 20% (v/v). Three independent experiments were done. Means and SEM are shown. *n* represents the number of experiments. *$p < 0,05$ for the indicated experimental points *versus* the corresponding untreated control.

To evaluate the mitogenic effect of NGF, BrdU incorporation and MTT assays were done in CRPC-derived cells. Exposure of C4-2B (Fig.1B), DU145 (Fig.1C) and PC3 (Fig.1D) cells to NGF resulted in a significant increase in BrdU incorporation. Remarkably, the stimulatory effect induced by NGF is comparable to that elicited by serum stimulation of all the CRPC cell lines. The TrkA inhibitor, GW441756 reverses the BrdU incorporation in PC cells stimulated with NGF, indicating that TrkA activity is required for this effect. GW441756 does not significantly modify the BrdU incorporation of cell lines, when used alone, as control. To reinforce the data obtained by BrdU incorporation, we also monitored cell proliferation by MTT assay. Consistent with findings obtained by BrdU analysis, MTT assay reveals that NGF treatment substantially stimulates the proliferation of all CRPC cell lines. Such stimulation started after 24h to reach the maximal effect

after 72h NGF-treatment (Fig. 1E-G). GW441756, which inhibits the NGF effect, does not impair the serum-induced proliferation, indicating its specific effect on NGF signaling (Fig. 1E-G).

Data in Fig. 1 show that TrkA activation by NGF drives the DNA synthesis and proliferation in C4-2B (Fig. 1B and E), DU145 (Fig.1C and F) and PC3 (Fig.1 D and G) cells.

2.2 NGF promotes migration and invasiveness of CRPC cells through TrkA activation.

We next assessed whether NGF triggers the motility of CRPC cells. Therefore, a wound scratch assay was firstly done. Quiescent C4-2B (panel A in Fig.2), DU145 (panel A in Fig.3) and PC3 (panel A in Fig.4) cells were wounded and then stimulated with NGF, in the absence or presence of GW441756.

Figure 2

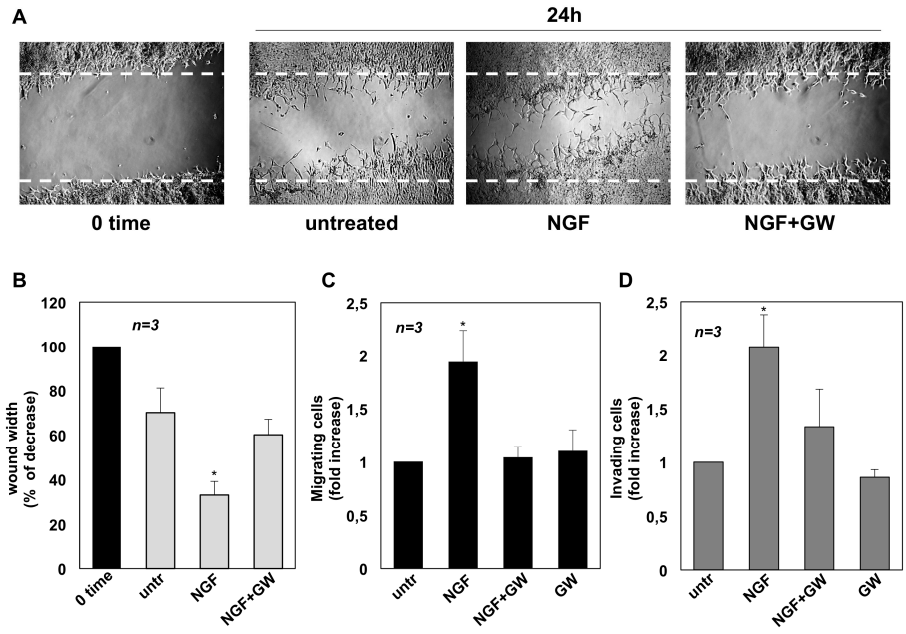

Figure 2. NGF triggers migration and invasiveness in C4-2B cells. In **A**, quiescent C4-2B cells were wounded and left untreated or treated with NGF for the indicated times. GW441756 (GW) was added at 1μM. Contrast-phase images are representative of 3 different experiments, each in duplicate. In (**B**), the wound area was measured using Leica Suite Software and data are presented as % in wound width over the control cells, analyzed at 0 time. Means and SEMs are shown. *n* represents the number of experiments. Quiescent C4-2B cells were used for migration (**C**) and invasion (**D**) assays in Boyden's chambers pre-coated with collagen or Matrigel, respectively. The indicated compounds were added to the upper and the lower chambers. NGF was used at 100 ng/ml and GW441756 (GW) at 1μM. After 7h (in **C**) or 24 h (in **D**), migrating or invading cells were counted as reported in Methods. Results from three different experiments were collected and expressed as fold increase. Means and SEMs are shown. *n* represents the number of experiments. *$p < 0,05$ for the indicated experimental points *versus* the corresponding untreated control.

Peer-reviewed version available at Cancers 2019, 11, 784; doi:10.3390/cancers11060784

Cells were allowed to migrate and contrast-phase images were acquired. They show that the wound gap is significantly reduced in C4-2B (Fig. 2A), DU145 (Fig. 3A) and PC3 (Fig. 4A) cells challenged with NGF. GW441756 inhibits the NGF-induced effect.

Figure 3

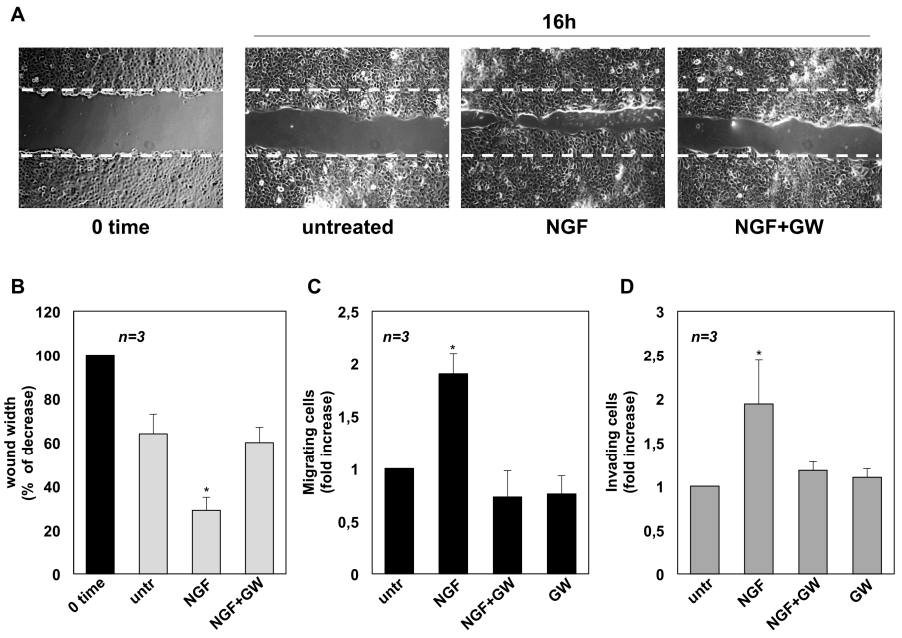

Figure 3. NGF triggers migration and invasiveness in DU145 cells. In **A**, quiescent DU145 cells were wounded and then left untreated or treated with NGF for the indicated time. When indicated, GW441756 (GW) was added at 1μM. Contrast-phase images are representative of 3 different experiments, each in duplicate. In (**B**), the wound area was measured as in Fig. 2 **B** and data are presented as % in wound width over the control cells, analyzed at 0 time. Means and SEMs are shown. *n* represents the number of experiments. Quiescent C4-2B cells were used for migration (**C**) and invasion (**D**) assays in Boyden's chambers pre-coated with collagen or Matrigel, respectively. The indicated compounds were added to the upper and the lower chambers. NGF was used at 100 ng/ml and GW441756 (GW) was used at 1μM. After 7h (**C**) or 24 h (**D**), cells were counted as reported in Methods. Results from three different experiments were collected and expressed as fold increase. Means and SEMs are shown. *n* represents the number of experiments. *$p < 0,05$ for the indicated experimental points *versus* the corresponding untreated control.

Preprints (www.preprints.org) | NOT PEER-REVIEWED | Posted: 11 April 2019 doi:10.20944/preprints201904.0142.v1

Peer-reviewed version available at Cancers 2019, 11, 784; doi:10.3390/cancers11060784

Figure 4

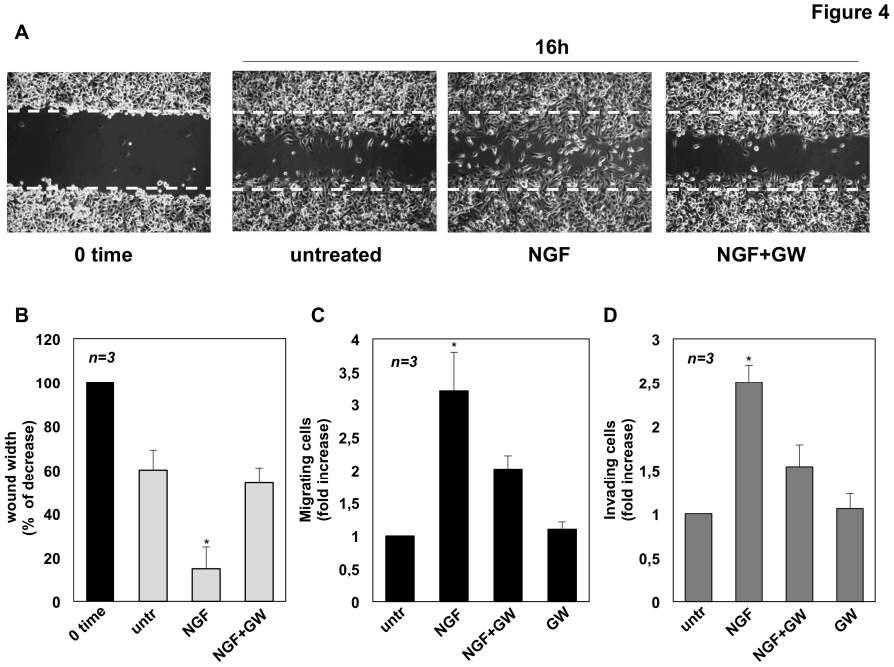

Figure 4. NGF triggers migration and invasiveness in PC3 cells. In **A**, quiescent PC3 cells were wounded and then left untreated or treated with NGF for the indicated times. GW441756 (GW) was added at 1μM . Contrast-phase images are representative of 3 different experiments, each in duplicate. In (**B**), the wound area was measured as in Fig. 2B and data are presented as % in wound width over the control cells analyzed at 0 time. Means and SEMs are shown. *n* represents the number of experiments. Quiescent C4-2B cells were used for migration (**C**) and invasion (**D**) assays in Boyden's chambers pre-coated with collagen or Matrigel, respectively. The indicated compounds were added to the upper and the lower chambers. NGF was used at 100 ng/ml and GW441756 (GW) was used at 1μM. After 7h (**C**) or 24 h (**D**), migrating or invading cells were counted as reported in Methods. Results from three different experiments were collected and expressed as fold increase. Means and SEMs are shown. *n* represents the number of experiments. *p < 0,05 for the indicated experimental points *versus* the corresponding untreated control.

Images captured at 0 time or from untreated cells are also shown for comparison. Results obtained from three different experiments are graphically presented in panel B of Figs. 2, 3 and 4 for C4-2B, DU-145 and PC3 cells, respectively. In the absence of any effect on cell proliferation (not shown), the wound gap is significantly ($p < 0,05$) reduced in cells treated with NGF, as compared with control, untreated cells. Here again, GW441756 reverses the effect of NGF in wound scratch assay.

We then analyzed the NGF effect on migration and invasiveness of CRPC cells using two additional assays. In collagen-coated Boyden's chamber transmigration assay, NGF increases by ~2-, 1,9- and 3,2-fold the number of C4-2B (Fig. 2C), DU145 (Fig. 3C) and PC3 (Fig. 4C) migrating cells, respectively. Here again, GW441756 significantly ($p < 0,05$) inhibits the NGF-induced effect, while it leaves almost unaffected the number of migrating cells, when used alone. Consistent with these results, significant changes in cell invasiveness were observed in Matrigel-coated Boyden's chamber

Peer-reviewed version available at Cancers 2019, 11, 784; doi:10.3390/cancers11060784

assay. Upon NGF challenging, indeed, the number of invading CRPC cells increases by ~2-fold in C4-2B (Fig. 2D) and DU145 (Fig. 3D) cells. A more robust effect by NGF (2,5-fold increase) is observed in PC3 cells (Fig. 4D), likely because integrins, which mediate cellular adhesion to extracellular matrix (ECM), are highly expressed in PC3 cells, as compared with C4-2B and DU145 cells. Addition of GW441756 significantly ($p < 0,05$) inhibits the NGF-induced invasiveness, while it scantly affects the number of invading cells when used alone, as a control.

Altogether, these findings indicate that TrkA activation by NGF promotes migration and invasiveness of CRPC cells in three different assays.

2.3 NGF promotes EMT of DU145 and PC3 cells through TrkA activation.

EMT positively affects tumor progression and metastatic spreading by enabling a switch from the stationary epithelial-like cell phenotype to the motile mesenchyme phenotype, with high ability to migrate, invade, and disorganize the extracellular matrix (ECM; [45] and therein refs). At molecular level, EMT is characterized by a decrease in the expression of epithelial markers, mainly E-cadherin, which is located to the cell surface of epithelial tissues, and an increase in the expression of mesenchyme markers, such as vimentin, a cytoskeleton protein associated with EMT initiation [46].

To investigate whether NGF stimulation triggers EMT in CRPC cells, quiescent cells were left untreated or treated for 72h with the indicated stimuli and lysate proteins were analyzed for expression of E-cadherin and vimentin. Regardless of stimuli, the Western blot analysis in Fig 5A (left panels) does not show significant changes in E-cadherin and vimentin levels in C4-2B cells. Similar findings were detected by densitometry analysis from three independent experiments (Fig. 1S, A and B).

Figure 5

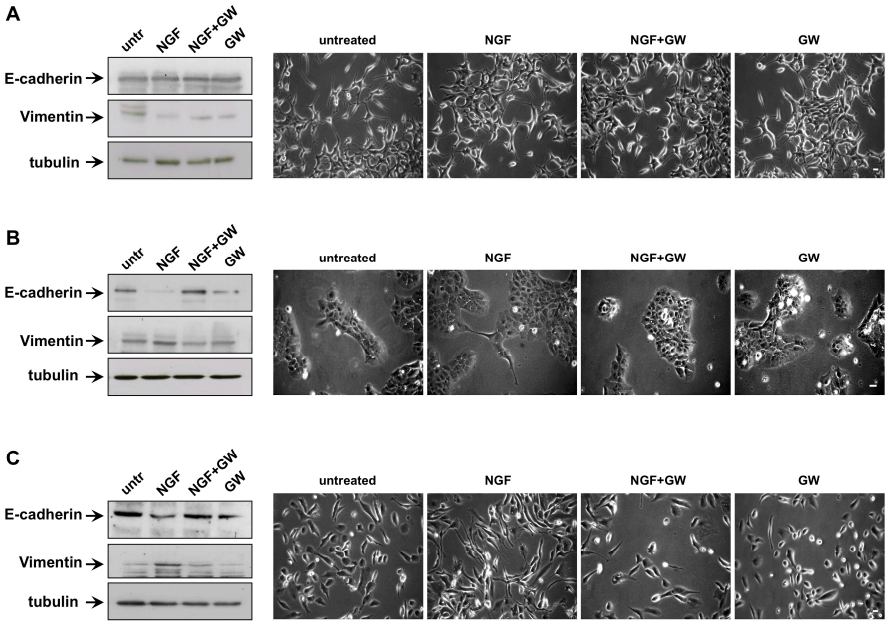

Figure 5. NGF promotes EMT in DU145 and PC3 cells. Quiescent C4-2B (**A**), DU145 (**B**) and PC3 (**C**) cells were left untreated or treated for 72h with the indicated

compounds. NGF was used at 100ng/ml and GW441756 (GW) at 1 μM. In **A-C** (left panels), lysate proteins were analyzed by Western blot, using the antibodies against the indicated proteins. The blots are representative of three different experiments. In **A-C** (right panels), contrast-phase images are representative of 3 different experiments, each in duplicate. Scale bar, 10 μm.

In the same experimental conditions, NGF treatment does not induce significant morphological changes in C4-2B cells, and similar findings were observed in cells treated with GW441756, alone or in combination with NGF (right panels in Fig. 5A). Quiescent DU145 cells (Fig. 5B) and PC3 (Fig. 5C) cells were then used. Here again, the cells were left untreated or treated for 72 h with the indicated compounds and lysates were analyzed for expression of E-cadherin and vimentin. NGF stimulation significantly down-regulates E-cadherin and up-regulates vimentin in both DU145 (Fig. 5B) and PC3 cells (Fig. 5C). Quantification of blots from three different experiments confirms these data (Fig. 1S, C and D, for DU145 cells; Fig. 1S, E and F for PC3 cells). GW441756 inhibits the NGF-elicited effect in both DU145 and PC3 cells, while it does not significantly modify E-cadherin and vimentin levels when used alone, as control in both cell lines (Fig. 5B and C; Fig 1S, C-F). We also locked at NGF-induced morphological changes of DU145 and PC3 cells. Images captured by contrast-phase microscopy show that 72h of NGF stimulation induces a rearrangement in DU145 (right panel in Fig. 5B,) and PC3 (right panel in Fig. 5C) cell shape from an orthogonal epithelial cell morphology (untreated, right panels in Fig. 5B and C), to a spindle-shaped fibroblast-like morphology (NGF-treated, right panels in Fig. 5B and C), reminiscent of cells having undergone EMT. GW441756 inhibits the NGF-induced effect in both cell lines, while it is ineffective when used alone, as control.

Data in Fig. 5 show that NGF robustly induces EMT in AR-negative DU145 and PC3 cells. In contrast, the NGF effect is almost undetectable in AR-positive C4-2B cells.
This behavior is consistent with the finding that NGF-challenged C4-2B cells migrate more slowly than DU145 and PC3 cells in our motility and invasion assays (Figs. 2, 3 and 4). Furthermore, C4-2B cells express high levels of E-cadherin and have high adherent junction functionality. In contrast, a decreased expression of epithelial markers and the appearance of epithelial phenotypic instability are required for responding to extracellular EMT inducers [47].

2.4 NGF increases CRPC 3D-organoid growth through TrkA activation.

Interactions between tumor cells and ECM are critical for cancer progression [48]. To develop cell culture models resuming cancer tissues and to reproduce more faithfully the complex architecture of tumors in *vivo*, 3D cultures were done. Contrast-phase images in Fig. 6 show that a 3D structure was observed in all CRPC cell lines used on 4 days of culture in ECM. Consistent with previous findings [49], C4-2B cells generated larger, less differentiated and irregular organoids, as compared with DU145 and PC3 cells. DU145 and PC3 cells generated, instead, a roundish and well-differentiated organoids. At that day-culture, organoids were untreated or treated with NGF, in the absence or presence of GW441756. Changes in dimension and structure of organoids were monitored for 14 days and contrast phase microscopy images were captured and shown (Fig. 6). Quantification of data was also done and graphically presented (Fig. 2S). After 14 days, NGF increases by about 4-, 7-

Peer-reviewed version available at Cancers 2019, 11, 784; doi:10.3390/cancers11060784

and 9-fold the size of C4-2B (upper panel in Fig.6, and Fig. 2S, A), DU-145 (middle panel in Fig.6 and Fig. 2S, B) and PC3 (lower panel in Fig. 6 and Fig. 2S, C) organoids, respectively. GW441756 significantly ($p < 0,05$ in Fig. 2S A, B and C) inhibits the NGF-induced effect. Again, images in Fig. 6 indicate that C4-2B cells form large, poorly differentiated organoids on 14 days of NGF treatment. In contrast, DU-145 cells undergo a transition from differentiated, round DU-145 organoids (basal condition) towards an invasive morphology when treated with NGF. Lastly, PC3 cells form round, well differentiated, and polarized spheroids, regardless of NGF stimulation.

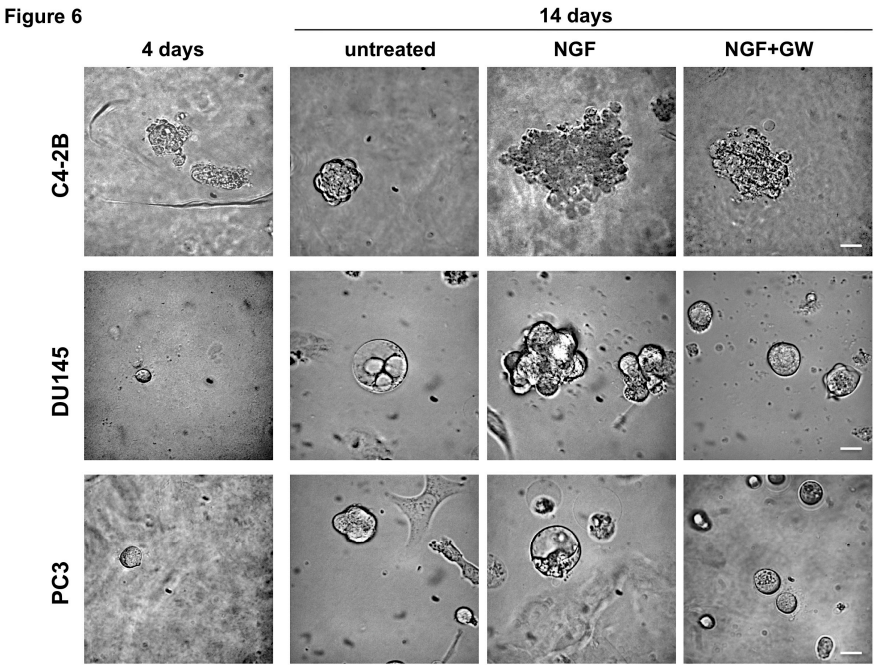

Figure 6. NGF increases the growth of organoids from CRPC cells through TrkA activation. C4-2B (upper panel), DU145 (middle panel) and PC3 (lower panel) were used in miniaturized 3D cultures in ECM, as reported in Methods. Four days after cells embedding in VitroGel-3D-RGD, representative images were acquired as described in Methods. 3D cultures were left untreated or treated with 100 ng/ml NGF, in the absence or presence of GW441756 (GW; 1 μM) for 14 days. Shown are contrast-phase images captured at 14th day. Scale bar, 100 μ

In addition to provide a valuable source for drug screening and more physiological information concerning the GW441756 inhibitory effect, findings in Figs. 6 and 2S demonstrate for the first time a key role for TrkA activation in the growth of CRPC-derived organoids, which recapitulate *in vitro* the tumor biology.

2.5 NGF triggers mitogen-activated protein kinases (MAPK) and Akt activation in CRPC cells.

The binding of NGF to TrkA activates its kinase domain, thereby triggering various downstream pathways, such as the MAPK [50,51] and the phosphoinositide 3-kinases (PI3-K)/Akt signaling cascade [31,52,53]. As readouts of NGF challenging, we analyzed MAPKs (ERK1 and 2) and Akt activation in a time course experiment. Quiescent CRPC cells were unstimulated or stimulated for the indicated times with NGF and lysate protein were analyzed by Western blot technique. A robust

Peer-reviewed version available at Cancers 2019, 11, 784; doi:10.3390/cancers11060784

ERK activation is observed in NGF-treated C4-2B cells, as compared with the weak Akt activation observed in the same experimental conditions. However, activation of both the effectors reached the maximal level within 5 minutes to decline within 15 and 30 min of NGF stimulation (Fig. 7A).

Figure 7

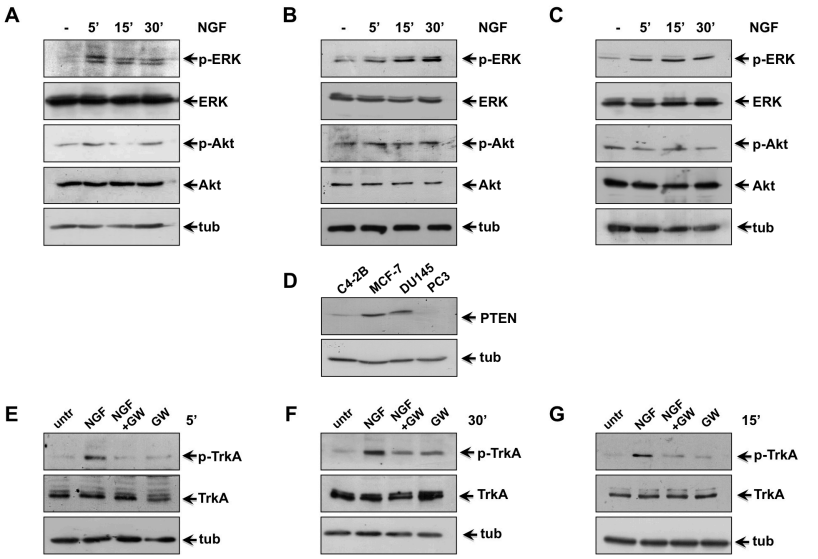

Figure 7. TrkA activation by NGF triggers MAPKs and Akt activation in CRPC cells. Quiescent C4-2B (**A** and **E**), DU145 (**B** and **F**) and PC3 (**C** and **G**) cells were used. In **A-C**, cells were left un-stimulated or stimulated for the indicated times with 100 ng/ml NGF. In **D**, the indicated cycling cells were used. In **E-G**, cells were left un-stimulated or stimulated for the indicated times with 100 ng/ml NGF, in the absence or presence of GW441756 (GW; 1μM). In **A-C,** lysate proteins were analyzed by Western blot, using the indicated antibodies (p-ERK stands for P-Tyr 204 ERK 1 and the corresponding phosphorylated ERK 2; p-Akt stands for P-Ser 473 Akt.) Filters were re-probed using anti ERK or anti Akt or anti tubulin (tub) antibodies, as a loading control. In (**D**), lysate proteins were analyzed by Western blot, using indicated antibdies. In **E-F**, lysate proteins were analyzed by Western blot, using the antibodies against the indicated proteins (p-TrkA stands for P-Tyr-490 TrkA).

Again, NGF stimulation induces a striking ERK activation and a slight Akt activation in DU-145 cells. ERK activation was observed already after 5 minutes of stimulation, with a stronger peak detectable after 30 minutes of treatment. Notably, Akt activation, if so, is very weak and delayed over the time, as compared with ERK activation. A slight P-Akt increase is detected only on 30 min NGF stimulation (Fig. 7B). At last, NGF stimulation induces ERK phosphorylation in PC3 cells, with an evident peak after 15 minutes of treatment. Remarkably, Akt activation is hardly to detect in NGF-treated cells (Fig.7C).

Densitometry analysis of immune-reactive bands detected by Western blot shows that the NGF-induced increase in ERK phosphorylation over the basal was about 3-, 5- and 2,5-fold in C4-2B (Fig. 3S, A), DU145 (Fig. 3S, C) and PC3 (Fig. 3S, E) cells, respectively. Furthermore, the

NGF-induced increase in Akt phosphorylation over the basal level was about 1,8- and 1,5-fold in C4-2B (Fig. 3S B) and DU145 (Fig. 3S D) cells, respectively. NGF did not modify the Akt activation status in PC3 cells (Fig. 3S, F). The loss of Akt modulation in PC3 cells is likely caused by the absence of PTEN, which is, instead, robustly expressed in MCF7 cells, analyzed as positive control. Appreciable levels of PTEN can be also detected in C4-2B and DU145 cells (Fig. 7D).

Albeit at different extent and timing, NGF induces a strong ERK activation in all the CRPC cell lines, accompanied by a weak Akt activation in C4-2B and DU-145 cells.

2.6 NGF triggers TrkA-Tyr-490 phosphorylation in CRPC cells.

We then investigated whether TrkA is the upstream event leading to NGF-induced ERK and Akt activation in CRPC cells. In addition to the tyrosine residues within the activation loop (Tyr-670, Tyr-674, and Tyr-675), TrkA exhibits two main tyrosine residues (Tyr-490 and Tyr-785), both outside the kinase domain. Once phosphorylated, these residues provide docking sites that lead to recruitment and activation of several signaling pathways [54,55].

Since MAPK and Akt pathway activation have been associated with Tyr-490 phosphorylation [56], we analyzed the NGF effect on Tyr490 phosphorylation of TrkA. Quiescent CRPC cells were left unchallenged or challenged for the indicated times with NGF, and P-Tyr490-TrkA phosphorylation was analyzed by Western blot technique. NGF treatment significantly increases P-Tyr-490 phosphorylation of TrkA in C4-2B (Fig. 7E), DU145 (Fig. 7F) and PC3 (Fig. 7G) cells, respectively. GW441756 inhibits the NGF-induced effect, while it leaves unaffected P-Tyr490 TrkA when used alone, as control (Fig. 7E-G). Altogether, findings in Figs. 7 and 3S suggest that Tyr-490 phosphorylation of TrkA represents the initial event activated by NGF in CRPC cells.

2.7 TrkA activation by NGF controls MAPKs and Akt activation in CRPC cells.

NGF-induced tyrosine phosphorylation of the TrkA receptor controls the subsequent activation of ERK or Akt [57]. Quiescent C4-2B (Fig. 8A), DU145 (Fig. 8B) and PC3 (Fig. 8C) cells were left unchallenged or challenged for the indicated times with NGF, in absence or presence of GW441756. The Western blots in Figure 8 show that NGF treatment significantly increases ERK activation. GW441756 inhibits such effect in all CRPC cells used, while it leaves almost unaffected ERK activation when used alone, as control (Fig. 8 A-C). Again, NGF treatment increases Akt activation in C4-2B (Fig. 8A) and in DU145 (Fig. 8B). Here again, GW441756 inhibits the NGF-induced effect, while it does not affect Akt activation when used alone, as control (Fig. 8 A-B). Consistent with data in Fig.7C, neither NGF, nor GW441756 modify Akt activation (Fig. 8C).

Preprints (www.preprints.org) | NOT PEER-REVIEWED | Posted: 11 April 2019 doi:10.20944/preprints201904.0142.v1

Peer-reviewed version available at Cancers 2019, 11, 784; doi:10.3390/cancers11060784

Figure 8

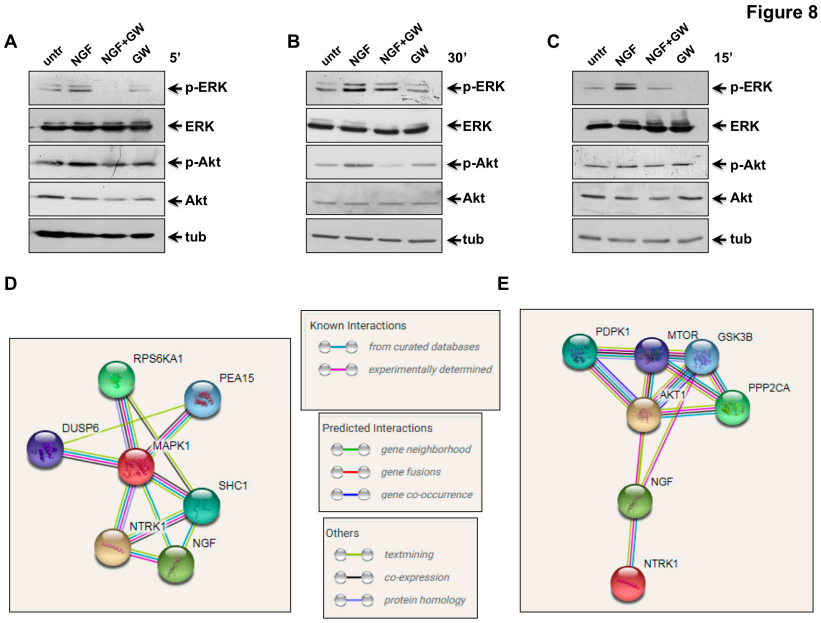

Figure 8. ERK and Akt are the downstream effectors of NGF/TrkA axis.
Quiescent C4-2B (**A**), DU145 (**B**) and PC3 (**C**) cells were used. In **A-C**, cells were left untreated (untr) or treated for the indicated times with NGF (100 ng/ml), in the absence or presence of 1μM GW441756. Lysates proteins were analyzed by Western blot, using the antibodies against the indicated proteins. (p-ERK stands for P-Tyr 204 ERK 1 and the corresponding phosphorylated ERK 2; p-Akt stands for P-Ser 473 Akt.) The filters were re-probed using anti ERK or anti Akt or anti tubulin (tub) antibodies, as loading controls. In **D-E**, the results from STRING network are shown. Combined screenshots from the STRING website, which has been queried with TrkA (NTRK1) and ERK (MAPK1; **D**) or TrkA (NTRK1) and Akt (AKT1; **E**) are shown**.** Colored lines between the proteins indicate the various type of interaction, as described in the middle section. Protein nodes also indicate the availability of 3D protein structure information.

By interrogating the String (Search Tool for the Retrieval of Interacting Genes/Proteins) database, which contains the known or predicted protein-protein interactions [58], we then constructed a network diagram for both TrkA (NTRK1) and ERK (MAPK1; Fig. 8D) as well as TrkA (NTRK1) and Akt (AKT1; Fig. 8E), respectively. Consistent with findings presented in panels A-C, these proteins belong to the same network through known or predicted interactions.

2.8 The role of MAPK and Akt activation in NGF-induced proliferation and migration of CRPC cells.

The role of NGF-induced activation of MAPK and Akt on CRPC cells proliferation and migration was then investigated using the PI-3K inhibitor, LY-294002 [59,60] as well as the MEKK inhibitor, PD98059 [31]. Expectedly, exposure of C4-2B (Fig. 9A), DU-145 (Fig. 9B) and PC3 (Fig. 9C) cells to NGF increases BrdU incorporation. LY-294002 prevents the NGF-elicited S-phase entry of C4-2B (Fig. 9A) and DU145 (Fig. 9B), while it does not modify the NGF-induced BrdU incorporation in PC3 cells (Fig. 9C). These results are consistent with the absence of PTEN in PC3 cells. LY-294002 doesn't

Peer-reviewed version available at Cancers 2019, 11, 784; doi:10.3390/cancers11060784

significantly affect BrdU incorporation of CRPC cells, when used alone. Albeit at different extent, PD98059 prevents the BrdU incorporation of C4-2B (Fig. 9A), DU145 (Fig. 9B) and PC3 (Fig. 9C) cells stimulated with NGF. The inhibitor doesn't significantly affect BrdU incorporation of DU145 and PC3 cells, while it significantly increases the proliferation of C4-2B cells when used alone, likely because MEK inactivation paradoxically removes an inhibition or leads to the simultaneous hyper-activation of PI3-K signalling in C4-2B cells.

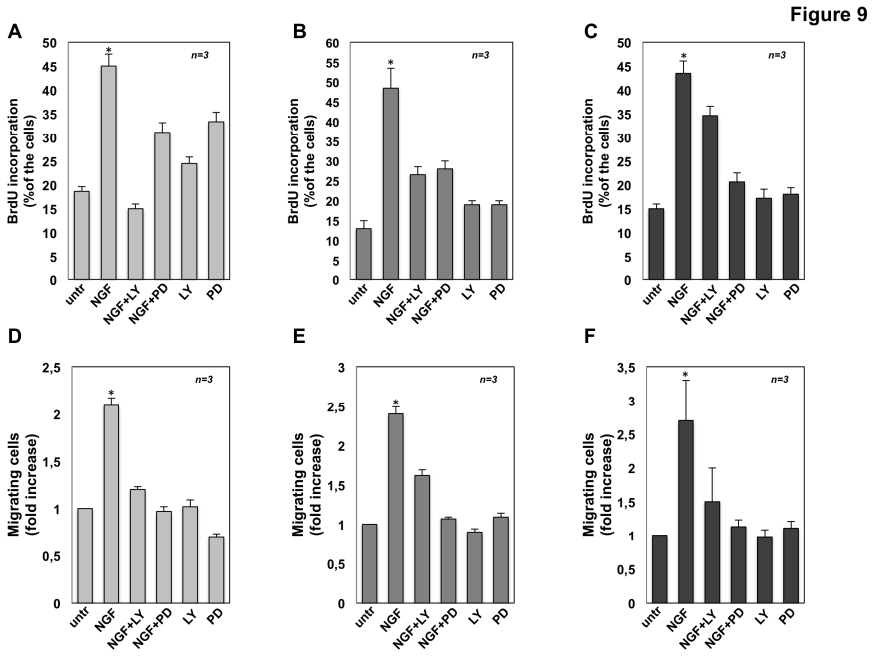

Figure 9. Inhibiton of Akt or ERK impairs the NGF-challenged proliferation and migration in CRPC cells.

C4-2B (**A**), DU145 (**B**) and PC3 (**C**) cells were left untreated (untr) or treated for 18h with the indicated compounds. After *in vivo* pulse with 100 μM BrdU, BrdU incorporation was analyzed by IF and expressed as % of total cells. C4-2B (**D**), DU145 (**E**) and PC3 (**F**) cells were used for migration assay in collagen pre-coated Boyden's chambers. The indicated compounds were added to the upper and the lower chambers. After 7h, migrated cells were counted as described in Methods and results expressed as fold increase. In **A-F**, NGF was used at 100 ng/ml; PD98059 (PD) and LY-294002 (LY) were used at 10 μM. Results from three different experiments have been collected. Means and SEMs are shown. *n* represents the number of experiments. *$p < 0,05$ for the indicated experimental points *versus* the corresponding untreated control

To evaluate the effect of LY-294002 and PD98059 on NGF-induced CRPC cell migration, collagen-coated Boyden's chambers were used. Both the inhibitors significantly impair the NGF-induced effect, while they leave almost unaffected the number of migrating cells, when used alone (Fig. 9 D-E).

Altogether, findings in Fig. 9 indicate that both Akt and MAPK activities are required for the NGF-induced S-phase entry and migration of CRPC cells. Noticeably, while the NGF migratory effect in CRPC cells is more sensitive to MEK inhibition, the NGF proliferative action is more sensitive to PI3-K inhibition, with the exception of PC3 cells. Thus, NGF utilizes PI3-K pathway to

Peer-reviewed version available at Cancers 2019, 11, 784; doi:10.3390/cancers11060784

transmit proliferative and survival signaling, while it engages MAPK circuit to activate the machinery involved in motility of CRPC cells.

3. Discussion

PC cells initially depend on androgens for their survival. This dependence, however, is progressively lost, leading to cancer spreading and resistance to androgen depletion therapies (ADT). At this stage, very limited therapeutic options are available in clinical practice ([33] and therein refs).

PC progression is accompanied by modifications in the expression of NGF and neurotrophin receptors [61,62]. These changes mainly consist in a reduction of p75NTR expression by the epithelial cells, in the absence of any significant modification in the expression of NGF or TrkA [63]. IHC studies in normal and malignant prostate epithelial tissue have substantially confirmed these findings [64]. To make this plot more complex, it has been also reported that PC cells aquire the ability to express neurotrophins as they progress[65]. All these findings point to the role of NGF/TrkA axis in sustaining PC progression and spreading.

In this paper, we have investigated the effect of NGF in various CRPC-derived cells. Among them, C4-2B cells express considerable amounts of AR, while DU-145 and PC3 are AR-negative. All the cell lines employed harbor significant levels of TrkA as well as ER , while they lack ER . Challenging of cells with NGF robustly increases Tyr-490 phosphorylation of TrkA. This event is upstream of NGF-induced ERK and/or Akt activation in CRPC cells. A significant increase of BrdU incorporation and cell proliferation then follows, as GW441756 similarly inhibits Tyr-490 phosphorylation of TrkA, and cell proliferation. The proliferative effect of NGF is similar in all cell lines employed and is reverted by TrkA inhibitor, GW441756. In addition to indicate that TrkA activation is required for MAPK as well as Akt activation and the consequent progression in cell cycle, these findings suggest that NGF can substitute androgens in sustaining the CRPC cell survival.

We next analyzed the NGF effect on cell motility and invasiveness by wound scratch and Trans-migration assays. Our data show that NGF consistently triggers cell motility and spreading in the cell lines employed. Notably, the effect of NGF is less impressive in C4-2B cells, as compared with that observed in DU-145 and PC3 cells. Consistent with these findings, C4-2B cells did not significantly undergo EMT on NGF challenging, while DU-145 and PC3 cells showed a significant increase in mesenchyme markers accompanied by a decrease in epithelial markers. These data are consistent with the concept that cells undergoing EMT become more motile [46]. Here again, GW441756 reverted the NGF effect, further corroborating its valuable effect in inhibiting PC spreading. Albeit at lower extent, C4-2B cells still migrate in the absence of EMT. These results are only apparently conflicting, since acquisition of a mesenchyme cell state is not a prerequisite of a migratory phenotype *in vitro* and *in vivo* [66]. Nevertheless, it might be hypothesized that AR expressed in C4-2B mitigates the NGF action. However, silencing of AR in C4-2B cells does not significantly modify the NGF effect on cell locomotion and invasiveness (not shown). It cannot be excluded that very small, traceable amounts of AR still interact with TrkA in NGF-treated C4-2B cells, thereby attenuating the ligand activation of basic machinery leading to cell spreading. A cross

Peer-reviewed version available at Cancers 2019, 11, 784; doi:10.3390/cancers11060784

457 talk between very low amounts of AR and TrkA leads to androgen-induced neuritogenesis in
458 neuronal cells [31]. A similar cross talk also regulates the NGF-elicited responses (proliferation and
459 motility) in androgen-sensitive LNCaP cells [32].
460
461 Organoid culture is largely accepted to study stem cells, organ development and patient-specific
462 diseases [67]. A standard protocol for organoid culture of human and mouse prostate epithelial and
463 PC tissues has been previously described [68]. However, the NGF effect on organoid growth of the
464 commonly used CRPC cell lines, C4-2B, PC3 and DU-145 has not been reported so far. In our study,
465 we followed the reported protocol [68] to set up organoid culture of CRPC cells. We found that
466 C4-2B, PC3 and DU-145 organoids were formed after 14-days culture in hydrogel and that NGF
467 significantly enhanced the growth of CRPC cells in 3D. Notably, GW441756 reverted the NGF effect
468 further suggesting that specific targeting of NGF/TrkA axis represents a very promising tool in
469 CRPC therapy.
470
471 Strategies aimed at inhibiting NGF signaling are already in clinical trials for the treatment of human
472 cancers, including PC. These therapies, however, frequently fail and induce side effects as well as
473 clinical resistance ([29,35] and therein refs). In addition to expanding our knowledge on the role of
474 NGF/TrkA axis in CRPC cells, our study provides a novel potential assay in 3D model to discover
475 new drugs for treating aggressive PC.
476
477

478 **4. Materials and Methods**

479

480 **4.1 Chemicals and reagents.**

481 NGF (Millipore) was used at 100 ng/ml. The TrkA inhibitor, GW441756 (Selleckchem) was added (at
482 1 μM, final concentration) 20 minutes before NGF stimulation. The mitogen-activated kinase kinase
483 (MEK) inhibitor PD98059 (Alexis, San Diego, CA) was added (at 10 μM, final concentration) 20
484 minutes before NGF stimulation. The PI-3K inhibitor, LY-294002 (Calbiochem) was added (at 10 μM,
485 final concentration) 30 minutes before NGF stimulation.
486

487 **4.2 Cell cultures.**

488 Human PC-derived DU145 cells were from Cell Bank Interlab Cell Line Collection (ICLC- Genova -
489 ITALY). Human PC-derived PC3 cells were a gift of Dr. P. Limonta (Department of Pharmacological
490 and Biomolecular Sciences, Università degli Studi di Milano, Milano, Italy). Human PC-derived
491 C4-2B cells were a gift of Dr G.N. Thalmann (Department of Urology, University Hospital Bern,
492 Bern, Switzerland). Cells were maintained at 37°C in humidified 5% CO_2 atmosphere. DU145 cells
493 were cultured in phenol-red DMEM containing 10% fetal bovine serum (FBS), penicillin (100 U/ml),
494 streptomycin (100 U/ml) and glutamine (2mM). Twenty-four hours before stimulation, growing
495 DU145 cells at 70% confluence were made quiescent using phenol red-free DMEM medium
496 containing penicillin (100 U/ml) and streptomycin (100 U/ml). PC3 cells were cultured in phenol-red
497 RPMI-1640/F12 containing 10% fetal bovine serum (FBS), penicillin (100 U/ml), streptomycin (100
498 U/ml) and glutamine (2mM). Forty-eight hours before stimulation, growing cells at 70% confluence

were made quiescent using phenol red-free RPMI-1640 medium supplemented with penicillin (100 U/ml), streptomycin (100 U/ml), and 0,5% charcoal-stripped serum (CSS). C4-2B cells were cultured in RPMI-1640 supplemented with 10% FBS, glutamine (2 mM), penicillin (100 U/ml), streptomycin (100 U/ml), sodium pyruvate (1 mM) and non-essential amino acids (10mM). Seventy-two hours before stimulation, growing cells at 70% confluence were made quiescent using phenol red-free RPMI-1640 medium containing 10% CSS, penicillin (100 U/ml), streptomycin (100 U/ml) and glutamine (2 mM). Media and supplements were from Gibco. Human BC-derived MCF-7 cells were from Cell Bank Interlab Cell Line Collection (ICLC- Genova - ITALY). Cells were maintained at 37°C in humidified 5% CO_2 atmosphere and cultured in phenol-red DMEM containing 10% fetal bovine serum (FBS), penicillin (100 U/ml), streptomycin (100 U/ml) and glutamine (2mM). The cell lines employed were routinely monitored for *Mycoplasma* contamination and expression of sex steroid receptors, as previously reported [69].

4.3 DNA synthesis, immunofluorescence (IF) microscopy and MTT assay.

Quiescent cells were left unchallenged or challenged with NGF (100ng/ml), in the absence or presence of the indicated compounds for 18h. After *in vivo* pulse with BrdU (100 M final concentration; Sigma-Aldrich), the BrdU incorporation into newly synthesized DNA was analyzed by IF microscopy, using a DMLB Leica (Leica) fluorescent microscope equipped with HCX PL Apo 63x oil objective, as reported [70]. The BrdU incorporation was calculated by the formula: percentage of BrdU-positive cells= (No. of BrdU-positive cells/No. of total cells) x 100. MTT assay was done using WST-1 reagent (Roche), as described [71]. Values were expressed as fold increase over the basal level.

4.4 Miniaturized 3D cultures in ECM.

The embedding method has been used to establish organoids for drug treatment experiments [72]. Briefly, cell suspension containing 5 x10^4 cells was mixed with 200 µl of VitroGel-3D-RGD (The Well Biosciences) for each well. The mixture was pipetted in 24-well plate as reported [73] and allowed to solidify for 45 min at 37°C, before the addition of 400 µl organoid plating medium to each well. Organoid plating medium was made as reported [68], using phenol red-free DMEM/F12 medium, containing 7% CSS, penicillin (100 U/ml), streptomycin (100 U/ml), diluted GlutaMAX 100X, 10 mM Hepes, B27 (50x stock solution), 1M nicotinamide, 500 mM N-acetylcysteine and 10 µM Y-27632 (Merck Millipore). After 3 days, the organoid plating medium was replaced with a similar medium without N-acetylcysteine and Y-27632. At the 4th day, organoids were untreated or treated with the indicated stimuli, in the absence or presence of inhibitors. The medium was changed every 3 days. Different fields were analyzed using DMIRB Leica (Leica) microscope equipped with C-Plan 20x objective (Leica). At the indicated times, contrast phase microscopy images were acquired using a DFC 450C camera (Leica) and the Application Suite Software (Leica). Images are representative of three independent experiments. The relative organoid size (area) was calculated using the Application Suite Software and expressed as a fold increase over the organoid area calculated at 4th day.

4.5 Wound scratch analysis, migration, invasiveness and contrast phase microscopy.

For wound scratch analysis, 1,8 x10^5 cells were seeded in a 24-well plate. Cells were made quiescent as above described and then wounded using 10µl sterile pipette tips. Cells were washed with PBS and then left un-stimulated or stimulated for the indicated times with NGF (100ng/ml), in the absence or presence of the indicated compounds. To avoid cell proliferation, cytosine arabinoside (Sigma-Aldrich) at 50 M (final concentration) was included in the cell medium. Different fields were analyzed using DMIRB inverted microscope (Leica) equipped with N-Plan 10x objective (Leica), as reported [74]. Contrast-phase images were captured using a DFC 450C camera (Leica) and acquired using Application Suite Software (Leica). Images are representative of at least three different experiments. The wound gap was calculated using Image J sofware and expressed as % of the decrease in the wound area. Migration assay was done using 3x10^4 cells in Boyden's chambers with 8 µm polycarbonate membrane (Falcon) pre-coated with collagen [75]. The indicated stimuli were added to the upper and the lower chambers. Cytosine arabinoside (at 50 M) was included in the cell medium. After 7h, non-migrating cells from the membrane upper surface were removed using a sterile cotton swab. Invasion assay was done using 5 x 10^4 cells in Boyden's chambers with 8 µm polycarbonate membrane (Falcon) pre-coated with growth factor reduced and phenol red-free Matrigel (Corning), as reported [75]. The indicated stimuli were added to the upper and the lower chambers. Here again, cytosine arabinoside (at 50 M) was included in the cell medium. After 24h, non-invading cells from the membrane upper surface were removed using a sterile cotton swab. In both, migration and invasiveness assays, the membranes were fixed for 20 min in 4% paraformaldehyde, stained with Hoechst, removed with forceps from the companion plate and mounted. Migrating or invading cells from at least 30 fields/each membrane were counted as described [75], using a DMLB (Leica) fluorescent microscope, equipped with HCPL Fluotar 20x objective. Data are representative of at least three different experiments.

4.6 EMT, lysates and Western blot technique.

EMT markers were analyzed by Western blot technique, as reported [76]. Briefly, quiescent cells were left un-stimulated or stimulated for the indicated times with NGF, in the absence or presence of GW441756 and then harvested in PBS containing 5 mM EDTA. Cell pellets were washed twice by centrifugation with PBS at 1,200 rpm and lysate proteins were prepared [76]. SDS-PAGE and Western blot techniques were done according to the same report. The rabbit polyclonal anti-vimentin (H-84; Santa Cruz) antibody was used to detect vimentin. The mouse monoclonal anti E-cadherin (clone 36/E, BD Biosciences) antibody was used to detect E-cadherin. AR was revealed as reported [69], using the mouse monoclonal anti-AR (441; Santa Cruz Biotechnology). The rabbit polyclonal anti-ERα (HC-20; Santa Cruz Biotechnology) and anti-ERβ (06-629, Millipore) antibodies were used to detect ER (or), respectively. The mouse monoclonal anti-tubulin antibody (Sigma-Aldrich) was used to detect tubulin. TrkA, ERK and Akt phosphorylation were analyzed as reported [31,32], using the rabbit polyclonal anti p-TrkA (Tyr-490; 9141S, Cell Signaling), or the mouse monoclonal anti p-ERK (sc-7383; Santa Cruz Biotechnology), or the rabbit polyclonal anti p-Akt (Ser-473; 9271S; Cell Signaling) antibodies. The rabbit polyclonal anti-TrkA (06-574; Millipore), or anti-ERK (C-14; Santa Cruz Biotechnology), or anti-Akt (9272; Cell Signaling) antibodies were used to detect TrkA, ERK and Akt, respectively. The ECL system (GE Healthcare) was used to reveal immune-reactive proteins.

Peer-reviewed version available at Cancers 2019, 11, 784; doi:10.3390/cancers11060784

585 **4.7 Analysis of network construction**

586 Network diagrams for protein-protein interaction analysis were generated with the use of STRING
587 (*Search Tool for the Retrieval of Interacting Genes software*; https://string-db.org/). Interaction prediction
588 was performed using the list of gene/protein names as a query. The results of this analysis yielded a
589 gene/protein interaction network, with the intensity of the edges reflecting the strength of the
590 interaction score, as reported in the legend. String database builds a protein-protein interaction
591 network for all of the required proteins [77].

592

593 **4.8 Statistical analysis**

594 All the experiments were performed in triplicate and data are presented as mean ± standard
595 deviation. Comparison for the different assays was evaluated with the paired two-tailed Student's
596 *t*-test. We used a *p* value of ≤0,05 indicative of statistical significance.

597

598 **5. Conclusions**

599

600 TrkA is involved in various cellular activities, mainly in neuritogenic and trophic signals [17-19].
601 Deregulation of TrkA is also a common feature of several cancer types, including PC [20, 23].

602

603 By activating TrkA and the downstream pathways (MAPK and Akt), NGF leads to proliferation,
604 invasiveness and EMT in three different CRPC cell lines. Moreover, NGF/TrkA axis promotes the
605 acquisition of a more aggressive phenotype in miniaturized 3D model. This approach offers
606 significant advantages over other systems for the study of PC features. Furthermore, in the era of
607 precision medicine, 3D model represents an invaluable tool to select compounds for a more tailored
608 management of metastatic CRPC.

609

610 Our findings warrant further prospective studies in 3D models from patients to validate the
611 reliability of TrkA as a biomarker to track and target in metastatic CRPC.

612

613

614 **Supplementary Materials:** The following are available online, Figure S1 **Densitometry analysis of**
615 **EMT markers expression in CRPC cells**; Figure S2 **Analysis of organoid size from CRPC cells**
616 **challenged with NGF;** Figure S3 **Densitometry analysis of ERK and Akt activation in CRPC cells.**

617

618 **Author Contributions:** M.D.D. and G.C. designed the study, performed the experiments and
619 analyzed the data; G.C. and A.M. wrote the manuscript. All the Authors approved the final draft of
620 the paper.

621

622 **Funding:** This work was supported by: Italian Ministry of University and Scientific Research
623 [P.R.I.N. 2015B7M39T_003 and P.R.I.N. 2017EKMFTN_002 to G.C.];
624 P.O.R - Regione Calabria [Progetto "Razionale" to A.M.].

Marzia Di Donato is supported by a fellowship of 'Fondazione Umberto Veronesi' [FUV Post-doctoral fellowship-2019].

Acknowledgments: We thank Dr. P. Limonta for PC3 cells and Dr. G.N. Thalmann for C4-2B cells.

Conflicts of Interest: The authors declare no conflict of interest. The funders had no role in the design of the study; in the collection, analyses, or interpretation of data; in the writing of the manuscript, or in the decision to publish the results.

References

1. Horwich, A.; Parker, C.; de Reijke, T.; Kataja, V.; ESMO Guidelines Working Group Prostate cancer: ESMO Clinical Practice Guidelines for diagnosis, treatment and follow-up. *Ann. Oncol.* **2013**, *24 Suppl 6*, vi106-114. doi:10.1093/annonc/mdt208
2. Leonel Almeida, P.; Jorge Pereira, B. Local Treatment of Metastatic Prostate Cancer: What is the Evidence So Far? *Prostate Cancer* **2018**, *2018*. doi:10.1155/2018/2654572
3. Carroll, P.R.; Parsons, J.K.; Andriole, G.; Bahnson, R.R.; Barocas, D.A.; Castle, E.P.; Catalona, W.J.; Dahl, D.M.; Davis, J.W.; Epstein, J.I.; et al. NCCN Clinical Practice Guidelines Prostate Cancer Early Detection, Version 2.2015. *J Natl Compr Canc Netw* **2015**, *13*, 1534–1561.
4. Ramamonjisoa, N.; Ackerstaff, E. Characterization of the Tumor Microenvironment and Tumor–Stroma Interaction by Non-invasive Preclinical Imaging. *Front. Oncol.* **2017**, *7*. doi:10.3389/fonc.2017.00003
5. Bergeret, S.; Charbit, J.; Ansquer, C.; Bera, G.; Chanson, P.; Lussey-Lepoutre, C. Novel PET tracers: added value for endocrine disorders. *Endocrine* **2019**. doi:10.1007/s12020-019-01895-z.
6. Calabria, F.; Chiaravalloti, A.; Cicciò, C.; Gangemi, V.; Gullà, D.; Rocca, F.; Gallo, G.; Cascini, G.L.; Schillaci, O. PET/CT with 18F-choline: Physiological whole bio-distribution in male and female subjects and diagnostic pitfalls on 1000 prostate cancer patients: 18F-choline PET/CT bio-distribution and pitfalls. A southern Italian experience. *Nucl. Med. Biol.* **2017**, *51*, 40–54. doi:10.1016/j.nucmedbio.2017.04.004.
7. Cuccurullo, V.; Di Stasio, G.D.; Evangelista, L.; Castoria, G.; Mansi, L. Biochemical and Pathophysiological Premises to Positron Emission Tomography With Choline Radiotracers. *J. Cell. Physiol.* **2017**, *232*, 270–275. doi:10.1002/jcp.25478.
8. Rapozzi, V.; Ragno, D.; Guerrini, A.; Ferroni, C.; Pietra, E. della; Cesselli, D.; Castoria, G.; Di Donato, M.; Saracino, E.; Benfenati, V.; et al. Androgen Receptor Targeted Conjugate for Bimodal Photodynamic Therapy of Prostate Cancer in Vitro. *Bioconjugate Chem.* **2015**, *26*, 1662–1671. doi:10.1021/acs.bioconjchem.5b00261.
9. Ahdoot, M.; Lebastchi, A.H.; Turkbey, B.; Wood, B.; Pinto, P.A. Contemporary treatments in prostate cancer focal therapy. *Curr Opin Oncol* **2019**. doi:10.1097/CCO.0000000000000515.
10. Migliaccio, A.; Castoria, G.; de Falco, A.; Bilancio, A.; Giovannelli, P.; Di Donato, M.; Marino, I.; Yamaguchi, H.; Appella, E.; Auricchio, F. Polyproline and Tat transduction peptides in the study of the rapid actions of steroid receptors. *Steroids* **2012**, *77*, 974–978. doi:10.1016/j.steroids.2012.01.014.

11. Tesei, A.; Leonetti, C.; Di Donato, M.; Gabucci, E.; Porru, M.; Varchi, G.; Guerrini, A.; Amadori, D.; Arienti, C.; Pignatta, S.; et al. Effect of small molecules modulating androgen receptor (SARMs) in human prostate cancer models. *PLoS ONE* **2013**, *8*, e62657. doi:10.1371/journal.pone.0062657.

12. Guerrini, A.; Tesei, A.; Ferroni, C.; Paganelli, G.; Zamagni, A.; Carloni, S.; Di Donato, M.; Castoria, G.; Leonetti, C.; Porru, M.; et al. A new avenue toward androgen receptor pan-antagonists: C2 sterically hindered substitution of hydroxy-propanamides. *J. Med. Chem.* **2014**, *57*, 7263–7279. doi:10.1021/jm5005122.

13. Warner, M.; Huang, B.; Gustaffson, J.A.. Estrogen Receptor β as a Pharmaceutical Target. *Trends in Pharmacological Sciences*, **2017** 38, 92-99 https://doi.org/10.1016/j.tips.2016.10.006

14. Di Zazzo, E.; Galasso, G.; Giovannelli, P.; Di Donato, M.; Di Santi, A.; Cernera, G.; Rossi, V.; Abbondanza, C.; Moncharmont, B.; Sinisi, A.A.; et al. Prostate cancer stem cells: the role of androgen and estrogen receptors. *Oncotarget* **2016**, *7*, 193–208. doi:10.18632/oncotarget.6220.

15. Di Zazzo, E.; Galasso, G.; Giovannelli, P.; Di Donato, M.; Castoria, G. Estrogens and Their Receptors in Prostate Cancer: Therapeutic Implications. *Front Oncol* **2018**, *8*. doi:10.3389/fonc.2018.00002.

16. Shen, M.M.; Abate-Shen, C. Molecular genetics of prostate cancer: new prospects for old challenges. *Genes Dev* **2010**, *24*, 1967–2000. doi:10.1101/gad.1965810.

17. Kaplan, D.R.; Miller, F.D. Neurotrophin signal transduction in the nervous system. *Curr. Opin. Neurobiol.* **2000**, *10*, 381–391.

18. Levi-Montalcini, R. oThe nerve growth factor 35 years later. *Science*. **1987** 237,1154-62. DOI: 10.1126/science.3306916

19. Murphy, R.A.; Watson, A.Y.; Rhodes, J.A. Biological sources of nerve growth factor. *Appl Neurophysiol* **1984**, *47*, 33–42.

20. Cunha, G.R.; Ricke, W.; Thomson, A.; Marker, P.C.; Risbridger, G.; Hayward, S.W.; Wang, Y.Z.; Donjacour, A.A.; Kurita, T. Hormonal, cellular, and molecular regulation of normal and neoplastic prostatic development. *J. Steroid Biochem. Mol. Biol.* **2004**, *92*, 221–236. doi:10.1016/j.jsbmb.2004.10.017.

21. Djakiew, D.; Pflug, B.; Onoda, M. Stromal-epithelial paracrine interactions in the neoplastic rat and human prostate. *Adv. Exp. Med. Biol.* **1993**, *330*, 185–202.

22. Delsite, R.; Djakiew, D. Characterization of nerve growth factor precursor protein expression by human prostate stromal cells: a role in selective neurotrophin stimulation of prostate epithelial cell growth. *Prostate* **1999**, *41*, 39–48.

23. Graham, C.W.; Lynch, J.H.; Djakiew, D. Distribution of nerve growth factor-like protein and nerve growth factor receptor in human benign prostatic hyperplasia and prostatic adenocarcinoma. *J. Urol.* **1992**, *147*, 1444–1447.

24. Geldof, A.A.; De Kleijn, M.A.; Rao, B.R.; Newling, D.W. Nerve growth factor stimulates in vitro invasive capacity of DU145 human prostatic cancer cells. *J. Cancer Res. Clin. Oncol.* **1997**, *123*, 107–112.

25. Walch, E.T.; Marchetti, D. Role of neurotrophins and neurotrophins receptors in the in vitro invasion and heparanase production of human prostate cancer cells. *Clin. Exp. Metastasis* **1999**, *17*, 307–314.

26. Weeraratna, A.T.; Dalrymple, S.L.; Lamb, J.C.; Denmeade, S.R.; Miknyoczki, S.; Dionne, C.A.; Isaacs, J.T. Pan-trk inhibition decreases metastasis and enhances host survival in experimental models as a result of its selective induction of apoptosis of prostate cancer cells. *Clin. Cancer Res.* **2001**, *7*, 2237–2245.

27. Festuccia, C.; Muzi, P.; Gravina, G.L.; Millimaggi, D.; Speca, S.; Dolo, V.; Ricevuto, E.; Vicentini, C.; Bologna, M. Tyrosine kinase inhibitor CEP-701 blocks the NTRK1/NGF receptor and limits the invasive capability of prostate cancer cells in vitro. *Int. J. Oncol.* **2007**, *30*, 193–200.

28. Arrighi, N.; Bodei, S.; Zani, D.; Simeone, C.; Cunico, S.C.; Missale, C.; Spano, P.; Sigala, S. Nerve growth factor signaling in prostate health and disease. *Growth Factors* **2010**, *28*, 191–201. doi:10.3109/08977190903578678.

29. Molloy, N.H.; Read, D.E.; Gorman, A.M. Nerve growth factor in cancer cell death and survival. *Cancers (Basel)* **2011**, *3*, 510–530. doi:10.3390/cancers3010510.

30. Warrington, R.J.; Lewis, K.E. Natural antibodies against nerve growth factor inhibit in vitro prostate cancer cell metastasis. *Cancer Immunol. Immunother.* **2011**, *60*, 187–195. doi:10.1007/s00262-010-0934-x

31. Di Donato, M.; Bilancio, A.; D'Amato, L.; Claudiani, P.; Oliviero, M.A.; Barone, M.V.; Auricchio, A.; Appella, E.; Migliaccio, A.; Auricchio, F.; et al. Cross-talk between androgen receptor/filamin A and TrkA regulates neurite outgrowth in PC12 cells. *Molecular Biology of the Cell* **2015**, *26*, 2858–2872. doi:10.1091/mbc.E14-09-1352.

32. Di Donato, M.; Cernera, G.; Auricchio, F.; Migliaccio, A.; Castoria, G. Cross-talk between androgen receptor and nerve growth factor receptor in prostate cancer cells: implications for a new therapeutic approach. *Cell Death Discov* **2018**, *4*, 5. doi:10.1038/s41420-017-0024-3.

33. Castoria, G.; Auricchio, F.; Migliaccio, A. Extranuclear partners of androgen receptor: at the crossroads of proliferation, migration, and neuritogenesis. *FASEB J.* **2017**, *31*, 1289–1300. doi:10.1096/fj.201601047R.

34. George, D.J.; Suzuki, H.; Bova, G.S.; Isaacs, J.T. Mutational analysis of the TrkA gene in prostate cancer. *Prostate* **1998**, *36*, 172–180.

35. Lange, A.M.; Lo, H.-W. Inhibiting TRK Proteins in Clinical Cancer Therapy. *Cancers (Basel)* **2018**, *10*. doi:10.3390/cancers10040105.

36. Thalmann, G.N.; Anezinis, P.E.; Chang, S.M.; Zhau, H.E.; Kim, E.E.; Hopwood, V.L.; Pathak, S.; von Eschenbach, A.C.; Chung, L.W. Androgen-independent cancer progression and bone metastasis in the LNCaP model of human prostate cancer. *Cancer Res.* **1994**, *54*, 2577–2581.

37. Thalmann, G.N.; Rhee, H.; Sikes, R.A.; Pathak, S.; Multani, A.; Zhau, H.E.; Marshall, F.F.; Chung, L.W.K. Human prostate fibroblasts induce growth and confer castration resistance and metastatic potential in LNCaP Cells. *Eur. Urol.* **2010**, *58*, 162–171. doi:10.1016/j.eururo.2009.08.026.

38. Kaighn, M.E.; Narayan, K.S.; Ohnuki, Y.; Lechner, J.F.; Jones, L.W. Establishment and characterization of a human prostatic carcinoma cell line (PC-3). *Invest Urol* **1979**, *17*, 16–23.

39. Stone, K.R.; Mickey, D.D.; Wunderli, H.; Mickey, G.H.; Paulson, D.F. Isolation of a human prostate carcinoma cell line (DU 145). *Int. J. Cancer* **1978**, *21*, 274–281.

40. Festuccia, C.; Gravina, G.L.; Muzi, P.; Pomante, R.; Ventura, L.; Ricevuto, E.; Vicentini, C.; Bologna, M. In vitro and in vivo effects of bicalutamide on the expression of TrkA and P75 neurotrophin receptors in prostate carcinoma. *Prostate* **2007**, *67*, 1255–1264. doi:10.1002/pros.20616.

41. Denmeade, S.R.; Sokoll, L.J.; Dalrymple, S.; Rosen, D.M.; Gady, A.M.; Bruzek, D.; Ricklis, R.M.; Isaacs, J.T. Dissociation between androgen responsiveness for malignant growth vs. expression of prostate specific differentiation markers PSA, hK2, and PSMA in human prostate cancer models. *Prostate* **2003**, *54*, 249–257. doi:10.1002/pros.10199.

42. Tilley, W.D.; Bentel, J.M.; Aspinall, J.O.; Hall, R.E.; Horsfall, D.J. Evidence for a novel mechanism of androgen resistance in the human prostate cancer cell line, PC-3. *Steroids* **1995**, *60*, 180–186.

43. Chlenski, A.; Nakashiro, K.; Ketels, K.V.; Korovaitseva, G.I.; Oyasu, R. Androgen receptor expression in androgen-independent prostate cancer cell lines. *Prostate* **2001**, *47*, 66–75. doi:10.1002/pros.1048.

44. Jung, E.J.; Kim, D.R. Apoptotic cell death in TrkA-overexpressing cells: kinetic regulation of ERK phosphorylation and caspase-7 activation. *Mol. Cells* **2008**, *26*, 12–17.

45. Hugo, H.; Ackland, M.L.; Blick, T.; Lawrence, M.G.; Clements, J.A.; Williams, E.D.; Thompson, E.W. Epithelial--mesenchymal and mesenchymal--epithelial transitions in carcinoma progression. *J. Cell. Physiol.* **2007**, *213*, 374–383. doi:10.1002/jcp.21223.

46. Thiery, J.P. Epithelial-mesenchymal transitions in tumour progression. *Nat. Rev. Cancer* **2002**, *2*, 442–454. doi:10.1038/nrc822.

47. Pistore, C.; Giannoni, E.; Colangelo, T.; Rizzo, F.; Magnani, E.; Muccillo, L.; Giurato, G.; Mancini, M.; Rizzo, S.; Riccardi, M.; et al. DNA methylation variations are required for epithelial-to-mesenchymal transition induced by cancer-associated fibroblasts in prostate cancer cells. *Oncogene* **2017**, *36*, 5551–5566. doi:10.1038/onc.2017.159

48. Friedl, P.; Alexander, S. Cancer invasion and the microenvironment: plasticity and reciprocity. *Cell* **2011**, *147*, 992–1009. doi:10.1016/j.cell.2011.11.016

49. Härmä, V.; Virtanen, J.; Mäkelä, R.; Happonen, A.; Mpindi, J.-P.; Knuuttila, M.; Kohonen, P.; Lötjönen, J.; Kallioniemi, O.; Nees, M. A comprehensive panel of three-dimensional models for studies of prostate cancer growth, invasion and drug responses. *PLoS ONE* **2010**, *5*, e10431. doi:10.1371/journal.pone.0010431.

50. Descamps, S.; Toillon, R.A.; Adriaenssens, E.; Pawlowski, V.; Cool, S.M.; Nurcombe, V.; Le Bourhis, X.; Boilly, B.; Peyrat, J.P.; Hondermarck, H. Nerve growth factor stimulates proliferation and survival of human breast cancer cells through two distinct signaling pathways. *J. Biol. Chem.* **2001**, *276*, 17864–17870. doi:10.1074/jbc.M010499200.

51. Gómez, N.; Cohen, P. Dissection of the protein kinase cascade by which nerve growth factor activates MAP kinases. *Nature* **1991**, *353*, 170–173. doi:10.1038/353170a0.

52. Ashcroft, M.; Stephens, R.M.; Hallberg, B.; Downward, J.; Kaplan, D.R. The selective and inducible activation of endogenous PI 3-kinase in PC12 cells results in efficient NGF-mediated survival but defective neurite outgrowth. *Oncogene* **1999**, *18*, 4586–4597. doi:10.1038/sj.onc.1202814.

53. Duan, L.; Hope, J.M.; Guo, S.; Ong, Q.; François, A.; Kaplan, L.; Scherrer, G.; Cui, B. Optical Activation of TrkA Signaling. *ACS Synth Biol* **2018**, *7*, 1685–1693. doi:10.1021/acssynbio.8b00126.

54. Kaplan, D.R.; Martin-Zanca, D.; Parada, L.F. Tyrosine phosphorylation and tyrosine kinase activity of the trk proto-oncogene product induced by NGF. *Nature* **1991**, *350*, 158–160. doi:10.1038/350158a0.

55. Van Kanegan, M.J.; Strack, S. The protein phosphatase 2A regulatory subunits B'beta and B'delta mediate sustained TrkA neurotrophin receptor autophosphorylation and neuronal differentiation. *Mol. Cell. Biol.* **2009**, *29*, 662–674. doi:10.1128/MCB.01242-08.

56. Obermeier, A.; Bradshaw, R.A.; Seedorf, K.; Choidas, A.; Schlessinger, J.; Ullrich, A. Neuronal differentiation signals are controlled by nerve growth factor receptor/Trk binding sites for SHC and PLC gamma. *EMBO J.* **1994**, *13*, 1585–1590.

794 57. Nakagawara, A. Trk receptor tyrosine kinases: a bridge between cancer and neural
795 development. *Cancer Lett.* **2001**, *169*, 107–114.
796 58. Jensen, L.J.; Kuhn, M.; Stark, M.; Chaffron, S.; Creevey, C.; Muller, J.; Doerks, T.; Julien, P.; Roth,
797 A.; Simonovic, M.; et al. STRING 8--a global view on proteins and their functional interactions in 630
798 organisms. *Nucleic Acids Res.* **2009**, *37*, D412-416. doi:10.1093/nar/gkn760.
799 59. Spear, N.; Estévez, A.G.; Barbeito, L.; Beckman, J.S.; Johnson, G.V. Nerve growth factor protects
800 PC12 cells against peroxynitrite-induced apoptosis via a mechanism dependent on
801 phosphatidylinositol 3-kinase. *J. Neurochem.* **1997**, *69*, 53–59.
802 60. Shimoke, K.; Kishi, S.; Utsumi, T.; Shimamura, Y.; Sasaya, H.; Oikawa, T.; Uesato, S.; Ikeuchi, T.
803 NGF-induced phosphatidylinositol 3-kinase signaling pathway prevents thapsigargin-triggered ER
804 stress-mediated apoptosis in PC12 cells. *Neurosci. Lett.* **2005**, *389*, 124–128.
805 doi:10.1016/j.neulet.2005.07.030.
806 61. Bostwick, DG.; Burke, HB.; Djakiew, D.; Euling, S.; Ho, SM; . Landolph, J.; Morrison, H.;
807 Sonawane, B.; Shifflett, T.; Waters, DJ.; Timms, B. Human prostate cancer risk factors. *Cancer.* **2004**
808 101, 2371-490 https://doi.org/10.1002/cncr.20408
809 62. Djakiew, D. Dysregulated expression of growth factors and their receptors in the development
810 of prostate cancer. *Prostate* **2000**, *42*, 150–160.
811 63. Krygier, S.; Djakiew D. Neurotrophin receptor p75(NTR) suppresses growth and nerve
812 growth factor-mediated metastasis of human prostate cancer cells. *Int J Cancer.* **2002,** 98,
813 1-7 https://doi.org/10.1002/ijc.10160
814 64. Graham, C.W.; Lynch, J.H.; Djakiew, D. Distribution of nerve growth factor-like protein and
815 nerve growth factor receptor in human benign prostatic hyperplasia and prostatic adenocarcinoma.
816 *J. Urol.* **1992**, *147*, 1444–1447.
817 65. Dalal, R.; Djakiew, D. Molecular characterization of neurotrophin expression and the
818 corresponding tropomyosin receptor kinases (trks) in epithelial and stromal cells of the human
819 prostate. *Mol Cell Endocrinol.* **1997** 134, 15-22. https://doi.org/10.1016/S0303-7207(97)00165-2
820 66. Schaeffer, D.; Somarelli, J.A.; Hanna, G.; Palmer, G.M.; Garcia-Blanco, M.A. Cellular migration
821 and invasion uncoupled: increased migration is not an inexorable consequence of
822 epithelial-to-mesenchymal transition. *Mol. Cell. Biol.* **2014**, *34*, 3486–3499. doi:10.1128/MCB.00694-14.
823 67. Gjorevski, N.; Sachs, N.; Manfrin, A.; Giger, S.; Bragina, M.E.; Ordóñez-Morán, P.; Clevers, H.;
824 Lutolf, M.P. Designer matrices for intestinal stem cell and organoid culture. *Nature* **2016**, *539*,
825 560–564. doi:10.1038/nature20168.
826 68. Drost, J.; Karthaus, W.R.; Gao, D.; Driehuis, E.; Sawyers, C.L.; Chen, Y.; Clevers, H. Organoid
827 culture systems for prostate epithelial and cancer tissue. *Nat Protoc* **2016**, *11*, 347–358.
828 doi:10.1038/nprot.2016.006.
829 69. Castoria, G.; Giovannelli, P.; Di Donato, M.; Ciociola, A.; Hayashi, R.; Bernal, F.; Appella, E.;
830 Auricchio, F.; Migliaccio, A. Role of non-genomic androgen signalling in suppressing proliferation
831 of fibroblasts and fibrosarcoma cells. *Cell Death & Disease* **2014**, *5*, e1548. doi:10.1038/cddis.2014.497.
832 70. Pagano, M. Control of DNA synthesis and mitosis by the Skp2-p27-Cdk1/2 axis. *Mol. Cell* **2004**,
833 *14*, 414–416.
834 71. Bilancio, A.; Bontempo, P.; Di Donato, M.; Conte, M.; Giovannelli, P.; Altucci, L.; Migliaccio, A.;
835 Castoria, G. Bisphenol A induces cell cycle arrest in primary and prostate cancer cells through

836 EGFR/ERK/p53 signaling pathway activation. *Oncotarget* **2017**, *8*, 115620–115631.
837 doi:10.18632/oncotarget.23360.
838 72. Chua, C.W.; Shibata, M.; Lei, M.; Toivanen, R.; Barlow, L.J.; Bergren, S.K.; Badani, K.K.;
839 McKiernan, J.M.; Benson, M.C.; Hibshoosh, H.; et al. Single luminal epithelial progenitors can
840 generate prostate organoids in culture. *Nat Cell Biol* **2014**, *16*, 951–4. doi:10.1038/ncb3047.
841 73. Beshiri, M.L.; Tice, C.M.; Tran, C.; Nguyen, H.M.; Sowalsky, A.G.; Agarwal, S.; Jansson, K.H.;
842 Yang, Q.; McGowen, K.M.; Yin, J.; et al. A PDX/Organoid Biobank of Advanced Prostate Cancers
843 Captures Genomic and Phenotypic Heterogeneity for Disease Modeling and Therapeutic Screening.
844 *Clin. Cancer Res.* **2018**, *24*, 4332–4345. doi:10.1158/1078-0432.CCR-18-0409.
845 74. Castoria, G.; D'Amato, L.; Ciociola, A.; Giovannelli, P.; Giraldi, T.; Sepe, L.; Paolella, G.; Barone,
846 M.V.; Migliaccio, A.; Auricchio, F. Androgen-induced cell migration: role of androgen
847 receptor/filamin A association. *PLoS ONE* **2011**, *6*, e17218. doi:10.1371/journal.pone.0017218.
848 75. Giovannelli, P.; Di Donato, M.; Auricchio, F.; Castoria, G.; Migliaccio, A. Androgens Induce
849 Invasiveness of Triple Negative Breast Cancer Cells Through AR/Src/PI3-K Complex Assembly. *Sci*
850 *Rep* **2019**, *9*, 4490. doi:10.1038/s41598-019-41016-4.
851 76. Rossi, V.; Di Zazzo, E.; Galasso, G.; De Rosa, C.; Abbondanza, C.; Sinisi, A.A.; Altucci, L.;
852 Migliaccio, A.; Castoria, G. Estrogens Modulate Somatostatin Receptors Expression and Synergize
853 With the Somatostatin Analog Pasireotide in Prostate Cells. *Front Pharmacol* **2019**, *10*, 28.
854 doi:10.3389/fphar.2019.00028.
855 77. Szklarczyk, D.; Morris, J.H.; Cook, H.; Kuhn, M.; Wyder, S.; Simonovic, M.; Santos, A.;
856 Doncheva, N.T.; Roth, A.; Bork, P.; et al. The STRING database in 2017: quality-controlled
857 protein-protein association networks, made broadly accessible. *Nucleic Acids Res.* **2017**, *45*,
858 D362–D368. doi:10.1093/nar/gkw937.